IOPscience iopscience.iop.org

Home Search Collections Journals About Contact us My IOPscience

An X-ray and NMR study of structure and ion motions in $C(NH_2)_3PF_6$

This article has been downloaded from IOPscience. Please scroll down to see the full text article.

1989 J. Phys.: Condens. Matter 1 7069

(http://iopscience.iop.org/0953-8984/1/39/019)

View the table of contents for this issue, or go to the journal homepage for more

Download details:
IP Address: 171.66.16.96
The article was downloaded on 10/05/2010 at 20:15

Please note that terms and conditions apply.

J. Phys.: Condens. Matter 1 (1989) 7069–7083. Printed in the UK

An x-ray and NMR study of structure and ion motions in $C(NH_2)_3PF_6$

M Grottel†, A Kozak‡, A E Kozioł§ and Z Pająk‡

† Department of Physics, Academy of Agriculture, 60–637 Poznań, Poland

‡ Institute of Physics, A Mickiewicz University, 60–780 Poznań, Poland

§ Institute of Chemistry, M Curie–Skłodowska University, 20-031 Lublin, Poland

Received 8 August 1988, in final form 23 January 1989

Abstract. A single-crystal x-ray analysis has shown that guanidinium hexafluorophosphate $C(NH_2)_3PF_6$ crystallises in the trigonal space group $R\bar{3}m$, with $a = 7.427(3)$ Å, $\alpha = 67.89(2)°$ and $Z = 2$. The guanidinium cation has the symmetry 3m (C_{3v}), the two inequivalent hexafluorophosphate anions $\bar{3}m$ (D_{3d}). The ions are connected by the weak N–H . . . F hydrogen bonds.

Proton and fluorine spin–lattice relaxation times as well as second moments have been measured over a wide range of temperatures. An analytical solution of a set of coupled differential equations describing the time variations of nuclear magnetisations was derived for four unlike spin systems. The analysis of all cross-relaxation effects enabled us to interpret the results in terms of C_3 reorientation of the cation and isotropic reorientation of two dynamically inequivalent anions. The activation parameters of the motions were found. The phase transitions and a convergence of cation and anion rotational correlation times at one of them (333 K) were discovered.

1. Introduction

Our interest in investigating ion motions in guanidinium salts led us recently to study guanidinium hexafluorophosphate, $C(NH_2)_3PF_6$, the compound suitable for NMR study of dynamics of both cation and anion sublattices.

By our precise x-ray analysis it was found that two PF_6 anions in the unit cell are not crystallographically equivalent, unlike the guanidinium cations. It seemed interesting to study both ion motions over a wide range of temperatures and to examine whether the structural inequivalence of the anions influences the dynamics of the ion sublattices. Moreover, the motional behaviour of the ions near phase transitions discovered by our NMR and DTA studies seemed also to be worth discussing.

In view of these questions, proton and fluorine NMR second moment as well as spin–lattice relaxation time T_1 as a function of temperature have been studied. In our work it was found experimentally that ^1H and ^{19}F spin–lattice relaxation became markedly non-exponential at most temperatures studied. To interpret the relaxation results we had to consider all cross-relaxation effects in the multi-spin system studied.

In our previous work (Kozak *et al* 1987) we succeeded in deriving the solution of a set of coupled differential equations describing the time variation of nuclear magnetisations for three unlike spins.

0953-8984/89/397069 + 15 $02.50 © 1989 IOP Publishing Ltd

Table 1. Final fractional coordinates and equivalent isotropic thermal parameters (Å^2). $U_{eq} = (U_{11} \times U_{22} \times U_{33})^{1/3}$.

Atom	Site symmetry	sof	x	y	z	U_{eq}
P(1)	$\bar{3}$m	1/12	0.0	0.0	0.0	0.0329(4)
P(2)	$\bar{3}$m	1/12	0.5	0.5	0.5	0.0350(4)
F(1)	m	1/2	0.1447(2)	0.1447(2)	−0.1281(3)	0.0469(6)
F(2)	m	1/2	0.5367(2)	0.5367(2)	0.2659(3)	0.0625(9)
C(1)	3m	1/6	0.2457(4)	0.2457(4)	0.2457(4)	0.0361(8)
N(1)	m	1/2	0.1535(3)	0.1535(3)	0.4279(5)	0.048(1)
H(1)	1	1	0.230(4)	0.046(4)	0.474(5)	0.075(10) (iso)
H(1)[a]			0.248	0.021	0.484	

[a] Corrected proton coordinates employed in the NMR calculations.

Table 2. Anisotropic thermal parameters. The temperature factor is of the form $\exp[-2\pi^2(U_{11}h^2a^{*2} + \ldots + 2U_{12}hka^*b^* + \ldots)]$.

Atom	U_{11}	U_{22}	U_{33}	U_{12}	U_{13}	U_{23}
P(1)	0.0329(7)	0.0329(7)	0.0329(7)	−0.0045(5)	−0.0045(5)	−0.0045(5)
P(2)	0.0350(7)	0.0350(7)	0.0350(7)	0.0005(5)	0.0005(5)	0.0005(5)
F(1)	0.0442(9)	0.0442(9)	0.053(1)	−0.018(1)	−0.0027(6)	−0.0027(6)
F(2)	0.081(1)	0.081(1)	0.037(1)	−0.002(2)	−0.0057(8)	−0.0057(8)
C(1)	0.036(1)	0.036(1)	0.036(1)	−0.009(1)	−0.009(1)	−0.009(1)
N(1)	0.052(1)	0.052(1)	0.042(2)	−0.007(2)	−0.006(1)	−0.006(1)

The dipolar interactions with fourth and fifth unlike spins occurring in the sample were only taken into account in the calculations of diagonal elements of the relaxation matrix.

In the present work we extend our theoretical approach to the cross-relaxation effect and present the solution of time behaviour of nuclear magnetisations for four unlike spins, i.e. ^{1}H, ^{19}F, ^{14}N and ^{31}P, between which dipolar interactions are considered.

2. X-ray investigation

2.1. Crystal data

Guanidinium hexafluorophosphate $CH_6N_3PF_6$, $M_w = 205.04$, trigonal space group R$\bar{3}$m, rhombohedral axes: $a = 7.427(2)$ Å, $\alpha = 67.89(2)°$, $V = 338.2(2)$ Å^3, $Z = 2$, $F(000) = 204$, μ(Mo Kα) = 3.96 cm^{-1}, $D_x = 2.01$ g cm^{-3}, $D_m = 2.02$ g cm^{-3} (by flotation in carbon tetrachloride + methyl iodide).

2.2. Structure determination and refinement

Colourless crystals of title salt were prepared by recrystallisation from a mixture of ethanol and water. The Laue symmetry ($\bar{3}$m) and the preliminary unit-cell dimensions

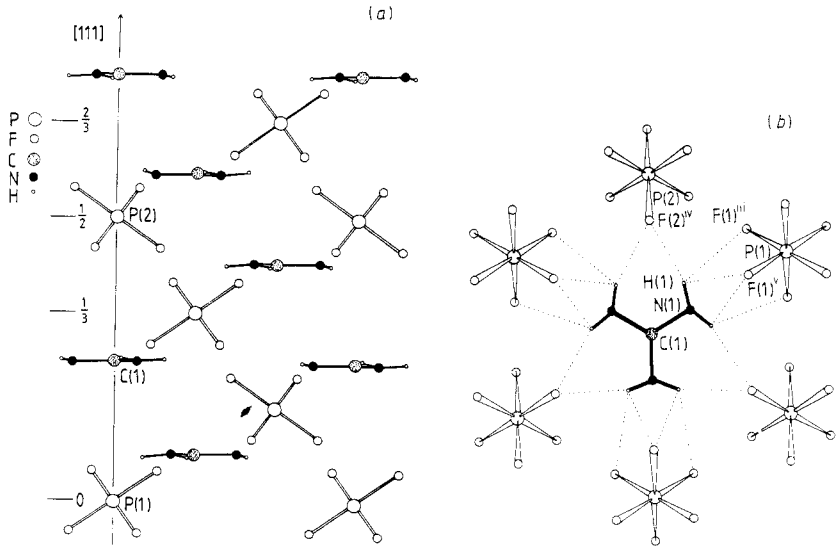

Figure 1. (*a*) Projection of crystal packing down the [1$\bar{1}$0] direction onto the mirror plane. (*b*) Projection down the [111] direction showing hydrogen bonds formed between the guanidinium cation and adjacent PF_6^- anions.

were obtained from Laue, oscillation and Weissenberg photographs. The cell parameters were subsequently refined using the setting angles of 15 reflections centred on a Syntex $P2_1$ diffractometer with Mo Kα radiation.

A single crystal of dimensions 0.20 × 0.24 × 0.39 mm was used for the diffraction-data collection in the $\theta/2\theta$ scan mode up to $2\theta_{max} = 55°$. The scan rate varied from 2.2 to 29.3° min^{-1}; the scan range was 2°. Intensities of 1747 reflections with *hkl* in the range h: $0 \rightarrow 7$, k: ± 8, l: ± 9 (one hemisphere) were recorded. Two standard reflections measured after every 50 reflections showed intensity variations of less than 6%. Lorentz and polarisation corrections were applied to the data; no correction was made for absorption. The reflections having $F_0/\sigma(F_0) \geq 2$ were considered, observed and used in calculations. Equivalent reflections were averaged to give 297 unique data points in the space group R$\bar{3}$m.

Patterson and Fourier syntheses were used to locate positions of non-hydrogen atoms. A difference map computed after the full-matrix least-squares refinement of non-H atom parameters gave the H-atom coordinates. Positional and thermal (anisotropic for non-H atoms and isotropic for H-atoms) parameters were refined. An isotropic extinction parameter x was included in the final stage of refinement; F_c is multiplied by $(1 - 0.001xF_c^2/\sin\theta)$, where $x = 0.010(2)$. Final discrepancy indices are $R = \Sigma|\Delta F|/\Sigma|F_0| = 0.0704$, $R_w = [\Sigma w(\Delta F)^2/\Sigma w(F_0)^2]^{1/2} = 0.0389$ (with $w = 1/\sigma^2$) and goodness-of-fit $[\Sigma w(\Delta F)^2/(NO - NV)]^{1/2} = 4.76$ (NO—number of observations, NV—number of parameters). The maximum shift for parameters in the last cycle of refinement was 0.005 σ. A final-difference map showed residual electron density in the range −0.34 to 0.42 e $Å^{-3}$. The highest peaks were located near the F(2) atom and had relatively large thermal amplitudes.

All calculations were carried out on a RIAD 32 computer with SHELX 76 system (Sheldrick 1976).

2.3. Results

The final positional and thermal parameters are listed in tables 1 and 2. The crystal structure is illustrated in figure 1. The intra- and inter-ionic dimensions are given in table 3. Figure 2 presents deviations of atoms from the least-squares plane calculated using three guanidinium nitrogen atoms. Figure 3 shows a stereoscopic view of the structure.

Lists of structure factors have been deposited with the British Library†.

2.4. Discussion

The rhombohedral symmetry of the guanidinium hexafluorophosphate crystal structure, $R\bar{3}m$, causes distortions of the possible idealised hexagonal symmetry $\bar{6}m2(D_{3h})$ of the guanidinium cation and the cubic symmetry $m\bar{3}m(O_h)$ of the PF_6^- anion. Thus, in the present structure the observed symmetry of cations is $3m(C_{3v})$, while positions of anions are centro-symmetric—$\bar{3}m(D_{3d})$. There are two chemical formulae in the unit cell. The guanidinium cations are related by the centres of symmetry. Two PF_6^- ions are symmetry-independent, both having the same point symmetry but different inter-ionic contacts.

Three equivalent C–N bonds in the $(C(NH_2)_3)^+$ cation are slightly shorter than those found in guanidinium perchlorate (1.327(4) Å) (Kozioł 1984) and tetrafluoroborate (1.322(6) Å) (Kozak *et al* 1987) structures, where the cation also adopts the symmetry 3m. Deviations of the C and H atoms from the plane through the guanidinium N atoms are about 3σ, so the cation is close to planar.

The P–F distances in PF_6^- groups are in good agreement with previously observed values (e.g. Thorup *et al* 1981, Castellano and Becker 1981, Wang *et al* 1980), and the F–P–F angles equal to 90° or 180° within experimental error. The difference of 0.011(4) Å between the P–F bond in the anion (1) and the anion (2) may be related to the different N–H . . . F hydrogen-bonding patterns involving these two anions.

The N–H residue acts as a triple donor. The F atoms of the anion (1) form two types of weak hydrogen bond; each F(1) atom interacts with four H atoms of guanidinium cations. The anion (2) is an acceptor of twelve equivalent hydrogen bonds (two bonds per each F(2) atom), which are stronger. The anion (1), participating in 24 hydrogen bonds, has a slightly longer P–F bond and a lower thermal motion than the anion (2).

The PF_6^- anions link parallel layers of cations to give a complex three-dimensional network of interacting ions. The scheme of inter-ionic hydrogen bonds observed in the centro-symmetric structure of guanidinium PF_6 is more complicated than that found in the polar structures (space group R3m) of isomorphous guanidinium ClO_4 and BF_4, in which two-dimensional interactions formed layers perpendicular to the threefold axis, and the H atom was involved in one single hydrogen bond.

3. NMR investigation

3.1. Experimental details

The guanidinium hexafluorophosphate obtained by allowing guanidinium carbonate to react with hexafluorophosphoric acid was recrystallised three times from an ethanol/

† Supplementary material to this paper is contained in a table of structure factors deposited with the British Library Publication Special Acquisitions and may be obtained from the British Library Document Supply Centre, Boston Spa, Wetherby, Yorkshire LS23 7BQ, UK, under reference number SUP 70038.

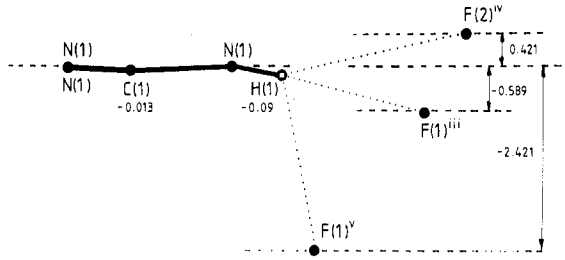

Figure 2. Deviations (Å) of atoms from the N_3 plane. Dotted lines show hydrogen bonds.

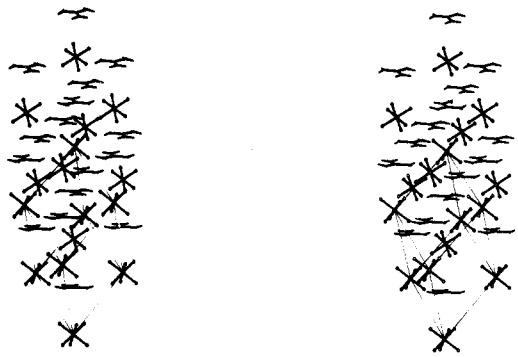

Figure 3. Stereoscopic view of the structure.

water solution. The product was then ground to powder and dried before being degassed and sealed off.

Measurements of the proton and fluorine NMR second moments (accuracy ± 10%) were carried out over a wide range of temperature, using a home-made wide-line spectrometer operating at Larmor frequencies of 28.0 and 26.3 MHz for protons and fluorines, respectively. The second-moment values were calculated by numerical integration of the first derivative of an absorption line and corrected for finite modulation amplitude (Andrew 1953). Mean values were obtained for about six derivatives registered at each temperature.

Measurements of proton and fluorine spin–lattice relaxation times (accuracy ± 7%) were performed as a function of temperature with 25 MHz and 38.2 MHz pulse spectrometers (Pająk *et al* 1974, Lewicki 1985) by a $\pi/2 - t - \pi/2$ pulse sequence.

The temperature of the sample was controlled by means of a gas-flow cryostat and monitored with a Pt resistor to an accuracy of 1 K.

All measurements were taken with increasing temperature, all calculations were performed using an Amstrad CPC 6128 computer.

Differential thermal analysis was made with Derivatograph type OD 102 system, from Hungary.

3.2. Results

Results of proton and fluorine NMR second-moment studies performed over a wide temperature range (130 to 403 K) are shown in figure 4. The proton second moment observed at lower temperatures (about 22.5 G^2) starts to decrease at about 160 K to the value of 4 G^2, achieved above 300 K. At about 400 K an abrupt decrease of the second

Table 3. Interatomic distances (Å) and angles (degrees), with estimated standard deviations in parentheses.

Symmetry code

none	x, y, z	iii	$-z, -x, 1-y$
i	z, x, y	iv	$1-y, -z, 1-x$
ii	y, x, z	v	$x, y, 1+z$

(a) Guanidinium cation

C(1)–N(1)	1.314(4)	C(1)–N(1)–H(1)	111(2)
N(1)–H(1)	0.82(3)	H(1)–N(1)–H(1)^{ii}	137(9)

(*b*) Hexafluorophosphate anions

P(1)–F(1)	1.596(2)	F(1)–P(1)–F(1)^{i}	90.3(8)
P(2)–F(2)	1.585(3)	F(2)–P(2)–F(2)^{i}	90.2(11)

(*c*) Hydrogen bonding

	N . . . F	H . . . F	<N–H . . . F
N(1)–H(1) . . . F(1)^{iii}	3.096(4)	2.61(4)	120(3)
N(1)–H(1) . . . F(2)^{iv}	3.084(3)	2.32(3)	155(3)
N(1)–H(1) . . . F(1)^{v}	3.249(5)	3.09(4)	94(3)

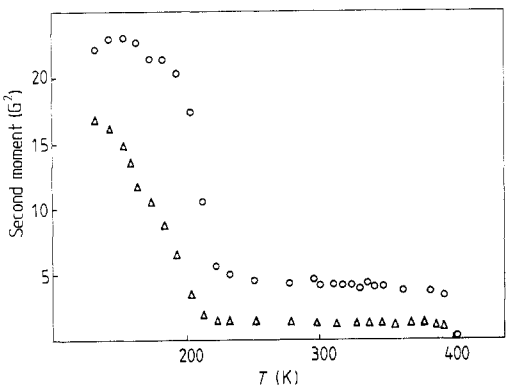

Figure 4. Temperature dependences of the proton (○) and fluorine (△) NMR second moments.

moment to a small value determined only by the field inhomogeneity (about 0.01 G^2) is observed. In the temperature interval 130–230 K the fluorine second moment changes from 16.7 G^2 to 1.2 G^2. The plateau value of 1.2 G^2 is observed up to 390 K, the temperature at which it starts to decrease. Figure 5 shows the temperature dependence of the fluorine linewidth and the shapes of three derivatives of the resonance lines registered at different temperatures. There is evidence of fine structure between 150 K and 195 K; hence two linewidth values are presented in figure 5.

The proton and fluorine spin–lattice relaxation times at the Larmor frequency of 25 MHz are shown as log T_1 plots against inverse temperature in figures 6 and 7, respectively. On the left-hand sides of both figures the relaxation times at 38.2 MHz are displayed in the extended scale for higher temperatures. The solid lines in the figures are theoretical fits to the experimental data described below in § 3.3.2. At most temperatures a non-exponential proton and fluorine magnetisation decay is observed. The

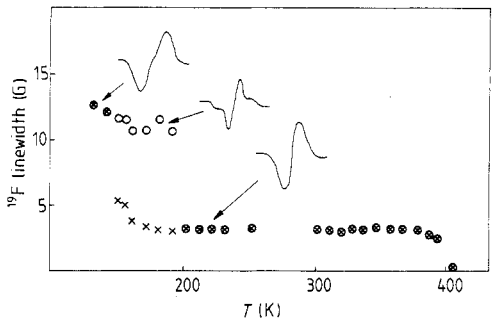

Figure 5. Temperature dependence of ^{19}F linewidth and the shapes of resonance-line derivatives for three different temperature regions.

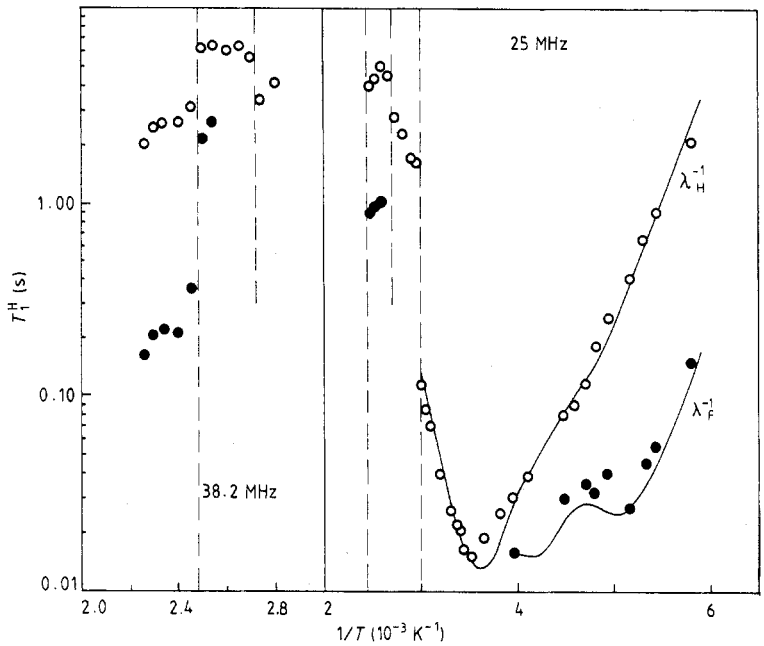

Figure 6. Temperature dependence of the proton spin–lattice relaxation time: ●, short; and ○, long components, when relaxation is non-exponential.

decay curves are decomposed into two exponential terms with different T_1 (see figure 8), yielding the results shown in figures 6 and 7. For protons relaxation becomes apparently one-exponential only between 260 and 370 K, while for fluorines, it does so at temperature interval 215 K–400 K. For protons there is a minimum at 283 K ($T_{1\min}^{H}$ = 15 ms), with different slopes of the curve at the low- and high-temperature sides.

For fluorines a minimum is found at 253 K ($T_{1\min}^{F}$ = 20 ms) and another one at about 200 K ($T_{1\min}^{F}$ = 24 ms). Typical semi-logarithmic plots of $(M_0 - M)/M_0$ against time for protons and fluorines at 193 K are given in figure 8.

Discontinuities in the temperature dependences of the proton and fluorine T_1 are observed at 333 K, 370 K and 401 K. At the same temperatures a preliminary DTA study has revealed an existence of phase transitions.

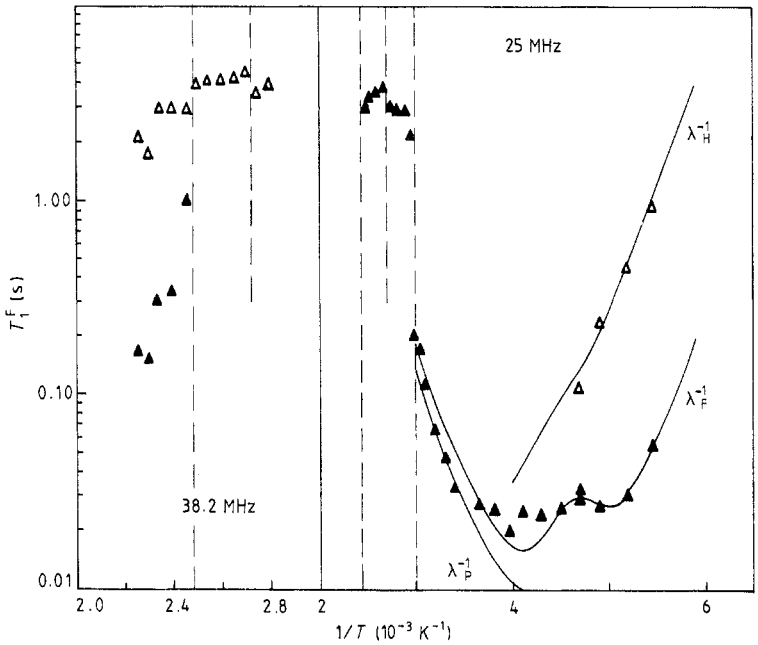

Figure 7. Temperature dependence of the fluorine spin–lattice relaxation time: ▲, short; and △, long components, when relaxation is non-exponential.

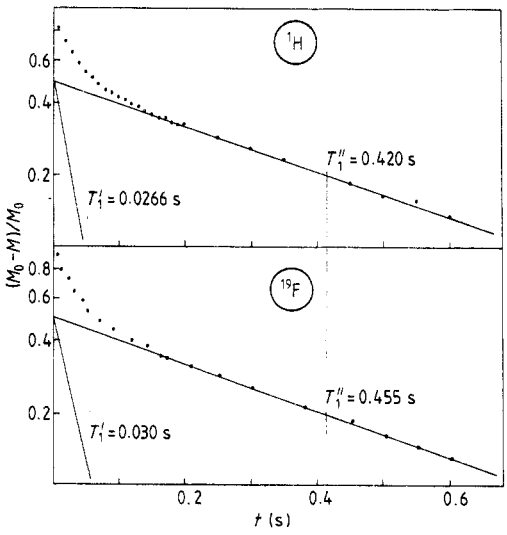

Figure 8. Typical plots of $(M_0 - M)/M_0$ against time for protons and fluorines at 193 K.

3.3. Calculations and discussion

3.3.1. NMR second moment. By using our x-ray data obtained for the guanidinium hexafluorophosphate we can calculate theoretical proton and fluorine second-moment values for a rigid lattice of the compound and for a few models of possible ion motions. Since an x-ray study does not reveal precise hydrogen atom positions in a crystal lattice (Schuster *et al* 1976) we had to make a correction for hydrogen coordinates as we did

Table 4. Second-moment values calculated for the rigid anion and cation sublattices of $C(NH_2)_3PF_6$.

	Second moment (G^2)				Second moment (G^2)		
Interaction	Intra-	Inter-	Total	Interaction	Intra-	Inter-	Total
		$C(NH_2)_3$ (1)				(PF_6) (1)	
H–H	15.09	1.67	16.76	F–F	9.91	1.32	11.23
H–N	2.05	0	2.05	F–P	1.56	0.01	1.57
H–F	0.13	2.80	2.93	F–H	0.15	2.34	2.49
H–P	0	0.03	0.03	F–N	0	0.01	0.01
			21.77				15.30
		$C(NH_2)_3$ (2)				(PF_6) (2)	
H–H	15.09	1.67	16.76	F–F	10.29	1.33	11.62
H–N	2.05	0	2.05	F–P	1.62	0.01	1.63
H–F	0.13	2.80	2.93	F–H	0.16	3.99	4.15
H–P	0	0.03	0.03	F–N	0	0.01	0.01
			21.77				17.41

previously (Kozak *et al* 1987, Grottel and Pająk 1984). The corrected values have been included in table 1.

The theoretical proton and fluorine second-moment values were found numerically, using the Van Vleck (1948) formula, taking into account in the calculations contributions from all kinds of magnetic nuclei occurring in the sample. Table 4 presents the proton and fluorine second-moment values obtained for rigid anion and cation sublattices. As one can see, structural inequivalence of the anions (1) and (2) leads to the different values of their second moments. The mean value for both anions is well comparable with the experimental one, registered at 130 K. For structurally equivalent cations we have also obtained a good agreement of the theoretical and experimental values of the second moments at temperatures lower than 160 K. Hence, at low temperatures, we can treat both ion sublattices as rigid in the NMR time-scale.

The theoretical second-moment values calculated for a few models of ion motions are presented in tables 5–8. From the temperature dependences of the proton and fluorine second moments it evidently follows that the anions start to reorient at lower temperatures than the cations. Furthermore, since the anions PF_6 (1) and PF_6 (2) are *not* structurally equivalent, being involved in a different number of hydrogen bonds and having different moments of inertia, we have had to discuss also possible difference in energy barriers to their reorientations. Hence in the first model we considered an isotropic reorientation of one PF_6 anion while the other anion and the guanidinium cation were still rigid. The values determined for this model of motion are shown in tables 5 and 6. Secondly, we calculated the second-moment values for the model of the simultaneous isotropic reorientations of both anions with the guanidinium cation still being rigid (table 7). Thirdly, we considered the model of the simultaneous isotropic reorientations of both anions together with the C_3 reorientation of the guanidinium cation (table 8).

The plateau value observed for the fluorine second moment at higher temperatures corresponds well to the isotropic reorientation of both PF_6 anions. However, the question arises as to whether or not both anions are set in motion simultaneously. A slightly

Table 5. Second-moment values calculated for isotropically reorienting PF_6 (1) with PF_6 (2) and $C(NH_2)_3$ rigid.

	Second moment (G^2)				Second moment (G^2)		
Interaction	Intra-	Inter-	Total	Interaction	Intra-	Inter-	Total
		$C(NH_2)_3$ (1)				(PF_6) (1)	
H–H	15.09	1.67	16.76	F–F	0	0.67	0.67
H–N	2.05	0	2.05	F–P	0	0	0.00
H–F	0.08	2.32	2.40	F–H	0.09	1.21	1.30
H–P	0	0.03	0.03	F–N	0	0.01	0.01
			21.24				1.98
		$C(NH_2)_3$ (2)				(PF_6) (2)	
H–H	15.09	1.67	16.76	F–F	10.29	0.77	11.06
H–N	2.05	0	2.05	F–P	1.62	0.01	1.63
H–F	0.13	2.26	2.39	F–H	0.16	3.99	4.15
H–P	0	0.03	0.03	F–N	0	0.01	0.01
			21.23				16.85

Table 6. Second moment values calculated for isotropically reorientating PF_6(2) with PF_6(1) and $C(NH_2)_3$ rigid.

	Second moment (G^2)				Second moment (G^2)		
Interaction	Intra-	Inter-	Total	Interaction	Intra-	Inter-	Total
		$C(NH_2)_3$ (1)				PF_6 (1)	
H–H	15.09	1.67	16.76	F–F	9.91	0.92	10.83
H–N	2.05	0	2.05	F–P	1.56	0.01	1.57
H–F	0.13	1.51	1.64	F–H	0.15	2.34	2.49
H–P	0	0.03	0.03	F–N	0	0.01	0.01
			20.48				14.90
		$C(NH_2)_3$ (2)				PF_6 (2)	
H–H	15.09	1.67	16.76	F–F	0	0.30	0.30
H–N	2.05	0	2.05	F–P	0	0.01	0.01
H–F	0.08	1.56	1.64	F–H	0.09	1.14	1.23
H–P	0	0.03	0.03	F–N	0	0.01	0.01
			20.48				1.55

marked two-step diminishing of the fluorine second moment would suggest an appearance of one anion reorientation at about 130 K and of the second one at about 160 K. It would produce a difference in energy barrier values of about 4 kJ mol^{-1}. To support the suggestion we show (figure 5) the temperature dependence of the linewidth and the shapes of the curves at three different temperatures. Between 150 and 190 K there is an evident appearance of a fine structure of the fluorine absorption lines. Two components of the NMR lines thus reflect two different mobilities of the inequivalent anions. The narrow line corresponds to the anion which has the lower energy barrier hindering its reorientation, the broad one to the anion with the higher energy barrier. While one anion reaches the reorientation frequency of 10^5 Hz at about 150 K, the other one only reaches the value at about 190 K. It is, however, difficult to decide which anion, PF_6 (1) or PF_6 (2) starts to reorient earlier.

Table 7. Second moment values calculated for isotropically reorienting $PF_6(1)$ and $PF_6(2)$ with $C(NH_2)_3$ rigid.

	Second moment (G^2)				Second moment (G^2)		
Interaction	Intra-	Inter-	Total	Interaction	Intra-	Inter-	Total
		$C(NH_2)_3(1)$				$PF_6(1)$	
H–H	15.09	1.67	16.76	F–F	0	0.54	0.54
H–N	2.05	0	2.05	F–P	0	0.01	0.01
H–F	0.08	1.04	1.12	F–H	0.09	1.21	1.30
H–P	0	0.03	0.03	F–N	0	0.01	0.01
			19.96				1.86
		$C(NH_2)_3(2)$				$PF_6(2)$	
H–H	15.09	1.67	16.76	F–F	0	0.12	0.12
H–N	2.05	0	2.05	F–P	0	0.01	0.01
H–F	0.08	1.04	1.12	F–H	0.09	1.14	1.23
H–P	0	0.03	0.03	F–N	0	0.01	0.01
			19.96				1.37

Table 8. Second moment values calculated for isotropically reorienting $PF_6(1)$ and $PF_6(2)$ and C_3 reorientation of $C(NH_2)_3$.

	Second moment (G^2)				Second moment (G^2)		
Interaction	Intra-	Inter-	Total	Interaction	Intra-	Inter-	Total
		$C(NH_2)_3(1)$				$PF_6(1)$	
H–H	3.77	0.63	4.40	F–F	0	0.54	0.54
H–N	0.48	0	0.48	F–P	0	0.01	0.01
H–F	0.04	0.52	0.56	F–H	0.05	0.58	0.63
H–P	0	0.02	0.02	F–N	0	0	0
			5.46				1.18
		$C(NH_2)_3(2)$				$PF_6(2)$	
H–H	3.77	0.63	4.40	F–F	0	0.54	0.54
H–N	0.48	0	0.48	F–P	0	0.01	0.01
H–F	0.04	0.52	0.56	F–H	0.05	0.58	0.63
H–P	0	0.02	0.02	F–N	0	0	0
			5.46				1.18

The second-moment reduction observed for protons from the value of 22.5 G^2 to about 4 G^2 can be interpreted in terms of a C_3 reorientation of the guanidinium cation. However, the theoretical second-moment value obtained for such a model of motion (5.5 G^2) is evidently higher than the experimental value (about 4 G^2) found at higher temperatures. It seems that apart from this type of reorientation there exists another one, already discussed (Kozak *et al* 1987), which further reduces the second moment.

A phase transition revealed at 333 K by the ^1H and ^{19}F relaxations as well as by DTA studies does not influence the second moments. On the contrary, a phase transition at about 400 K slightly indicated in both the relaxation and the DTA studies is clearly manifest by an abrupt decrease of the second moment to a liquid-like value, suggesting a transition to a new solid phase wherein an ion self-diffusion occurs in the crystal lattice.

3.3.2. NMR relaxation time. The experimental proton and fluorine relaxation times (T_1^H and T_1^F) of polycrystalline guanidinium hexafluorophosphate presented in figures 6 and 7, show rather complicated temperature dependences. The lower-temperature ($T < 200$ K) two-exponential behaviour of T_1^H and T_1^F is typical for cross-relaxation effect in a system of two unlike spins ^{1}H and ^{19}F (Caron *et al* 1967). Such an effect is observed particularly when the difference between the spin angular frequencies $\omega_H - \omega_F \simeq 9$ MHz is comparable with an inverse of the correlation time of the molecular reorientation $\tau \geqslant 0.1$ μs. As the compound studied contains not only spins ^{1}H and ^{19}F but also two others, namely ^{31}P and ^{14}N, one must consider a cross-relaxation effect in a four-unlike-spin system. The quadrupolar contribution from ^{14}N may be neglected because of the reorientations of both ions (Abragam 1961) as also may be the dipolar contributions from ^{13}C and ^{15}N owing to their very small abundance.

In our previous work (Kozak *et al* 1987) we derived an analytical solution of a set of coupled differential equations describing a time variation of nuclear magnetisations for three unlike spins. The dipolar interactions with the fourth and fifth dissimilar spins were considered only in the calculations of diagonal elements of the relaxation matrix. Here, in the case of guanidinium hexafluorophosphate, for the dipolar interactions between four unlike spins the total relaxation matrix should be considered:

$$[R] = \begin{bmatrix} -R_{HH} & -R_{HF} & -R_{HP} & -R_{HN} \\ -R_{FH} & -R_{FF} & -R_{FP} & -R_{FN} \\ -R_{PH} & -R_{PF} & -R_{PP} & -R_{PN} \\ -R_{NH} & -R_{NF} & -R_{NP} & -R_{NN} \end{bmatrix}.$$

Following the convention for $C(NH_2)_3BF_4$ (Kozak *et al* 1987) we can present the equation of motion for magnetisation in the form

$$[\dot{M}] = -[R][M - M_0] \tag{1}$$

wherein $[M]$ is a columnar matrix of the magnetisations corresponding to nuclei ^{1}H, ^{19}F, ^{31}P and ^{14}N, respectively, while $[M_0]$ is a columnar matrix of the equilibrium values of those magnetisations.

A general solution of equation (1) is

$$[M] = \exp([R]t)\,([M(0)] - [M_0]) + [M_0] \tag{2}$$

where $[M(0)]$ is a columnar matrix of the nuclear magnetisations at $t = 0$. Expanding $\exp(Rt)$ into a series by using the Sylvester formula (Fröberg 1974) and assuming $\pi/2$–t–$\pi/2$ pulse sequence in the experiment we get the following expression for the time behaviour of the ith magnetisation:

$$\frac{M_{0i} - m_i}{M_{0i}} = \sum_{r=1}^{4} A_{ir} \exp(\lambda_r t) \tag{3}$$

where $\lambda_1 \neq \lambda_2 \neq \lambda_3 \neq \lambda_4$ are eigenvalues of the R matrix. The amplitudes of the magnetisations, A_{ir}, connected with the respective eigenvalues, λ_r, we calculated from the formulae

$$A_{ir} = \prod_{m \neq r} (\lambda_m - \lambda_r)^{-1} \left[\prod_{m \neq r} (\lambda_m + R_{ii}) + \sum_{k \neq i} R_{ik} R_{ki} \left(\sum_{m \neq r} \lambda_m + 2R_{ii} + R_{kk} \right) + \sum_{k \neq i \neq n \neq p} R_{ik}(R_{kn} R_{ni} + R_{kp} R_{pi}) \right] \tag{4}$$

where subscripts i, k, n, p are here ascribed to four different spin systems. Though the expressions (4) are somewhat more complicated than those found for a system of three unlike spins, they are very useful for predicting the magnetisation behaviour for the cases of various molecular motions. The explicit form of the amplitude describing the proton magnetisation connected with λ_1 is the following:

$$\begin{aligned} A_{H1} = [(\lambda_2 - \lambda_1)(\lambda_3 - \lambda_1)(\lambda_4 - \lambda_1)]^{-1}[&(\lambda_2 + R_{HH})(\lambda_3 + R_{HH})(\lambda_4 + R_{HH}) \\ &+ R_{HF}R_{FH}(\lambda_2 + \lambda_3 + \lambda_4 + 2R_{HH} + R_{FF}) + R_{HP}R_{PH}(\lambda_2 + \lambda_3 + \lambda_4 \\ &+ 2R_{HH} + 2R_{PP}) + R_{HN}R_{NH}(\lambda_2 + \lambda_3 + \lambda_4 + 2R_{HH} + R_{NN}) \\ &+ R_{HF}(R_{FN}R_{NH} + R_{FP}R_{PH}) + R_{HP}(R_{PF}R_{FH} + R_{PN}R_{NH}) \\ &+ R_{HN}(R_{NP}R_{PH} + R_{NF}R_{FH})]. \end{aligned} \tag{5}$$

The same form will do for other spin magnetisations or other eigenvalues of the relaxation matrix.

Remembering that cross-relaxation becomes important in the temperature ranges in which $\omega_i \pm \omega_k \simeq 1/\tau$, we can expect in our case of $B_0 \simeq 0.6$ T an evident non-exponential magnetisation decay resulting from following interactions:

^1H–^{19}F			for $\tau > 10^{-7}$ s
^1H–^{14}N, ^1H–^{19}F, ^{19}F–^{31}P	or	^{19}F–^{14}N	for 10^{-9} s $< \tau < 10^{-7}$ s
^{19}F–^{31}P, ^1H–^{31}P	or	^1H–^{19}F	for $\tau < 10^{-9}$ s.

It is noteworthy that a superposition of all four different interactions occurs in the vicinity of the observed reorientational minima of the relaxation times ($\omega\tau \simeq 0.6$).

To describe the time behaviour of the proton and fluorine magnetisations for a wide range of temperatures we have first to calculate the relaxation-matrix elements for an assumed model of both ion reorientations. Our discussion of the second-moment results has shown that the C_3 reorientation of the cation and the isotropic reorientation of the anions take place in the compound investigated. Hence the following relaxation matrix should be considered:

$$R = R_H + R_F \tag{6}$$

where R_H and R_F are the relaxation matrices for the cation and the anion reorientations, respectively. However, since the anions (1) and (2) are structurally inequivalent, we considered also their different mobilities, putting

$$R = R_H + \tfrac{1}{2}R_{F(1)} + \tfrac{1}{2}R_{F(2)}. \tag{7}$$

We calculated the diagonal and off-diagonal elements of the relaxation matrix using the formulae

$$R_{II} = \tfrac{2}{3}\gamma_I^2 \Delta M_2^{II} g_1(\omega_I, \tau) + \tfrac{1}{2}\sum_S \gamma_I^2 \Delta M_2^{IS} g_2(\omega_I, \omega_S, \tau)$$

where

$$g_1(\omega_I, \tau) = \tau/(1 + \omega_I^2\tau^2) + 4\tau/(1 + 4\omega_I^2\tau^2),$$

$$g_2(\omega_I, \omega_S, \tau) = \tau/[1 + (\omega_I - \omega_S)^2\tau^2] + 3\tau/(1 + \omega_I^2\tau^2) + 6\tau/[1 + (\omega_I + \omega_S)^2\tau^2]$$

$$R_{IS} = \tfrac{1}{2}\gamma_S^2 \Delta M_2^{SI} g_3(\omega_I, \omega_S, \tau)$$

Table 9. Activation parameters for the motions considered.

Type of motion	E_a (kJ mol^{-1})	τ_0 (s)
Isotropic reorientation		
anion (1)	23.5 ± 1.2	(3.50 ± 0.13) × 10^{-14}
anion (2)	27.4 ± 1.3	(1.13 ± 0.06) × 10^{-14}
C_3 reorientation		
cation	43.2 ± 2.1	(3.75 ± 0.16) × 10^{-17}

where

$$g_3(\omega_I, \omega_S, \tau) = -\tau/[1 + (\omega_I - \omega_S)^2\tau^2] + 6\tau/[1 + (\omega_I + \omega_S)^2\tau^2]$$

where the correlation time τ describes the C_3 reorientation of the cation (τ_H) or the isotropic reorientation of the anions ($\tau_{F(1)}$ and $\tau_{F(2)}$). Assuming both reorientations to be thermally activated, we have calculated the λ_H^{-1}, λ_F^{-1}, λ_P^{-1} and λ_N^{-1} values, as well as the respective amplitudes of magnetisation for the ^{1}H and ^{19}F resonances occurring simultaneously. The calculated values were fitted to the respective experimental data, employing as fitting constants the Arrhenius activation energies (E_a^H, $E_a^{F(1)}$, $E_a^{F(2)}$) and pre-exponential factors τ_0^H, $\tau_0^{F(1)}$, $\tau_0^{F(2)}$). The best fitted activation parameters are listed in table 9.

The solid lines depicted in figures 6 and 7 present the inverses of the calculated eigenvalues for all spins considered whose contribution to the proton and/or the fluorine relaxation is higher than 2%. The small contributions do not affect the apparent one-exponential magnetisation decay observed in the experiment, though they influence the measured T_1 values, which then do not exactly correspond to the inverses of respective eigenvalues. This is probably the reason for the poor agreement observed for λ_F^{-1} near the minimum slightly below 250 K. Except for this temperature region for fluorines, one can see a satisfactory agreement between theoretical and experimentally observed T_1^H and T_1^F values over a wide range of temperatures.

The analysis performed of the cross-relaxation effects in the four-spin system of the compound under study has shown that apparently complicated temperature dependences of ^{1}H and ^{19}F relaxation times can be reasonably interpreted in terms of a relatively simple model of the ion motions. The procedure enabled us to confirm the existence of a C_3 reorientation of the guanidinium cation as well as of the isotropic reorientation of the anions. The activation energy for the cation is comparable to the values found for the guanidinium tetrafluoroborate and perchlorate, thus also reflecting weak H-bonding effects. The structural inequivalence of the hexafluorophosphate anions results in their different dynamics—the mobility of the PF_6 (1) anion appears higher than that of PF_6 (2) anion. However, the lower value of the pre-exponential factor for the PF_6 (2) anion points to its higher thermal oscillations, in agreement with our x-ray results. The procedure also made possible the determination of the correlation times characterising the ion motions in the low-temperature phase of the compound. It turns out that the log τ against $1/T$ plots shown in figure 9 converge (within the accuracy limit) just at the first-order phase transition (333 K) where rotational correlation times for the cation and both anions reach a common value of about 10^{-10} s. This fact points to the existence of a new kind of coupling of rotational modes of the cation and anion

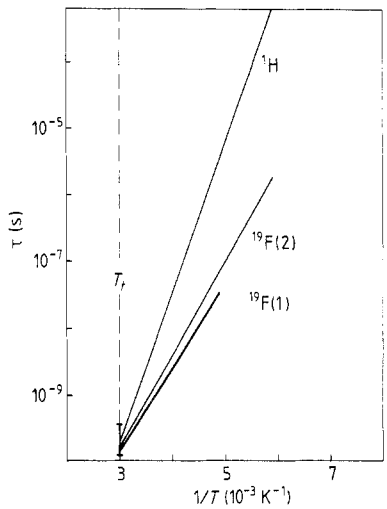

Figure 9. Temperature dependence of the correlation times for the guanidinium cation and both PF_6 anions.

sublattices. This effect, which we also discovered in the other guanidinium salts, has been discussed and reported earlier (Pająk *et al* 1988).

Acknowledgment

The research was supported by the Polish Academy of Sciences under Project CPBP 01.12.

References

Abragam A 1961 *The Principles of Nuclear Magnetism* (Oxford: OUP) p 295
Andrew E R 1953 *Phys. Rev.* **91** 425
Caron A P, Huettner D J, Ragle J L, Sherk L and Stengle T R 1967 *J. Chem. Phys.* **47** 2577
Castellano E E and Becker R W 1981 *Acta Crystallogr.* B **37** 61
Fröberg C E 1974 Introduction to Numerical Analysis (London: Addison–Wesley) p 66
Grottel M and Pająk Z 1984 *J. Chem. Soc. Faraday Trans.* II **80** 553
Kozak A, Grottel M, Kozioł A E and Pająk Z 1987 *J. Phys. C: Solid State Phys.* **20** 5433
Kozioł A E 1984 *Z. Kristallogr.* **168** 313
Lewicki S 1985 *PhD Thesis* A Mickiewicz University, Poznań
Pająk Z, Jurga K and Jurga S 1974 *Acta Phys. Pol.* A **45** 837
Pająk Z, Kozak A and Grottel M 1988 *Solid State Commun.* **65** 671
Schuster P, Zundel G and Sandorfy C 1976 *The Hydrogen Bond* (Amsterdam: North-Holland)
Sheldrick G M 1976 SHELX 76 (Program for crystal structure determination) University of Cambridge, UK
Thorup N, Rindorf G, Soling H and Bechgaard K 1981 *Acta Crystallogr.* B **37** 1236
Van Vleck J H 1948 *Phys. Rev.* **74** 1168
Wang Y, Calvert L D and Brownstein S K 1980 *Acta Crystallogr.* B **36** 1523